

EDISON

Electromagnetic Design of
flexible Sensors



Parametrized local model order reduction

Martyna Mul
August 22, 2019



The „EDISON - Electromagnetic Design of flexibleSensOrs”project, agreement no TEAM TECH/2016-1/6, is carried out within the TEAM-TECH programme of the Foundation for Polish Science co-financed by the European Union under the European Regional Development Fund.

Revision	Date	Author(s)	Description
1.0	22.08.2019	M. Mul	created

1 Introduction

The behavior of the electromagnetic field in subdomain Ω_i is described by the local system of equations:

$$(\mathbf{\Gamma}_{\Omega_i} - k^2 \mathbf{C}_{\Omega_i}) \cdot \mathbf{E}_{\Omega_i} = -(\mathbf{G}_{\delta\Omega_i} - k^2 \mathbf{T}_{\delta\Omega_i}) \cdot \mathbf{E}_{\delta\Omega_i} \quad (1)$$

where $\mathbf{G}_{\delta\Omega_i}$ and $\mathbf{T}_{\delta\Omega_i}$ are blocks that couple the subregion Ω_i and the artificial boundary $\delta\Omega_i$, \mathbf{E}_{Ω_i} is associated with FE basis functions in Ω_i and $\mathbf{E}_{\delta\Omega_i}$ contains coefficients associated with FE basis functions on the boundary $\delta\Omega_i$.

Here we can define a local transfer function that describes the input-output behavior in subdomain Ω_i :

$$\mathbf{H}_{\Omega_i}(k) = -(\mathbf{G}_{\delta\Omega_i}^T - k^2 \mathbf{T}_{\delta\Omega_i}^T) \cdot (\mathbf{\Gamma}_{\Omega_i} - k^2 \mathbf{C}_{\Omega_i})^{-1} \cdot (\mathbf{G}_{\delta\Omega_i} - k^2 \mathbf{T}_{\delta\Omega_i}) \quad (2)$$

Note that the poles of the local transfer function defined above are the same as the eigenvalues of the matrix pencil $(\mathbf{\Gamma}_{\Omega_i}, \mathbf{C}_{\Omega_i})$.

Next, local model order reduction is applied. The projection space \mathbf{Q} is found and the Galerkin projection is applied to the system 1. Model order reduction results in the reduced system of equations:

$$(\tilde{\mathbf{\Gamma}}_{\Omega_i} - k^2 \tilde{\mathbf{C}}_{\Omega_i}) \cdot \tilde{\mathbf{E}}_{\Omega_i} = -(\tilde{\mathbf{G}}_{\delta\Omega_i} - k^2 \tilde{\mathbf{T}}_{\delta\Omega_i}) \cdot \mathbf{E}_{\delta\Omega_i}, \quad (3)$$

where

$$\begin{aligned} \tilde{\mathbf{\Gamma}}_{\Omega_i} &= \mathbf{Q}^T \mathbf{\Gamma}_{\Omega_i} \mathbf{Q}, \\ \tilde{\mathbf{C}}_{\Omega_i} &= \mathbf{Q}^T \mathbf{C}_{\Omega_i} \mathbf{Q}, \\ \tilde{\mathbf{G}}_{\delta\Omega_i} &= \mathbf{Q}^T \mathbf{G}_{\delta\Omega_i}, \\ \tilde{\mathbf{T}}_{\delta\Omega_i} &= \mathbf{Q}^T \mathbf{T}_{\delta\Omega_i}, \\ \mathbf{E}_{\Omega_i} &= \mathbf{Q} \tilde{\mathbf{E}}_{\Omega_i}. \end{aligned} \quad (4)$$

The reduced form of the local transfer function $\tilde{\mathbf{H}}_{\Omega_i}$ is defined as follows:

$$\tilde{\mathbf{H}}_{\Omega_i}(k) = -(\tilde{\mathbf{G}}_{\delta\Omega_i}^T - k^2 \tilde{\mathbf{T}}_{\delta\Omega_i}^T) \cdot (\tilde{\mathbf{\Gamma}}_{\Omega_i} - k^2 \tilde{\mathbf{C}}_{\Omega_i})^{-1} \cdot (\tilde{\mathbf{G}}_{\delta\Omega_i} - k^2 \tilde{\mathbf{T}}_{\delta\Omega_i}) \quad (5)$$

The local projection basis \mathbf{Q} is computed using approach described in [1]. In this report the results of analysis using parametrized model order reduction are shown. The simulation scheme is as follows:

- The projection basis \mathbf{Q}_0 is generated for the starting (initial) set of design parameters \mathbf{p}_0 .
- New set of design parameters \mathbf{p} is chosen and mesh is deformed.
- Projection basis \mathbf{Q}_0 is used to solve for the new geometry instead of generating a new one from scratch.
- The projection basis is modified by adding new vectors to the projection space: \mathbf{V} representing accurate poles of the local transfer function defined in (2) and \mathbf{S} representing field solution of the local system of equation at the specified frequency (1). As a result, the local projection basis \mathbf{Q}_p is created which is composed of three parts:

$$\mathbf{Q}_p = [\mathbf{Q}_0, \mathbf{V}, \mathbf{S}]. \quad (6)$$

2 Results

Two numerical examples were considered - dual mode waveguide filter and 5th order waveguide filter with dispersive couplings. Both narrowband and wideband analyses have been made.

2.1 Dual mode circular waveguide filter - narrowband analysis

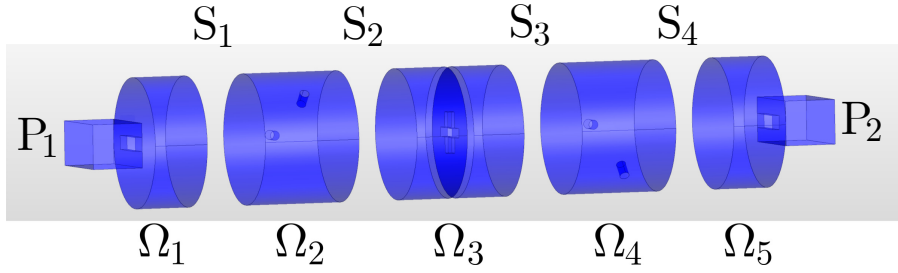


Figure 1: Structure of the filter and segmentation scheme

The structure was partitioned into 5 macroelements: Ω_1 , Ω_2 , Ω_3 , Ω_4 , Ω_5 and 2 ports and 4 cross-sections: P_1 , P_2 , S_1 , S_2 , S_3 , S_4 as depicted in Fig. 1.

The number of unknowns in ports and cross-sections was reduced by applying the modal projection technique. The number of modes used for modal projection is shown in Table 2.

interface	number of modes	
	TE	TM
P_1	2	2
P_2	2	2
S_1	24	17
S_2	24	17
S_3	24	16
S_4	24	17

Table 2: Number of modes used for the modal projection on ports.

Initial results with PMOR

Figure 2 shows the scattering parameters computed when initial parametrized local ROMs were applied. In all of three macromodels, the single projection basis was used. There is also the actual error of the analysis defined as: $|S_{PMOR} - S_{MP}|$, where S_{MP} stands for the scattering parameters computed prior to the reduction process (and after applying the modal projection on ports) and S_{PMOR} is the result of the analysis using PMOR.

Values of the parameter set under analysis (\mathbf{p}) as well as values of parameters \mathbf{p}_0 that were used to construct the initial projection basis \mathbf{Q}_0 are given in Table 3 .

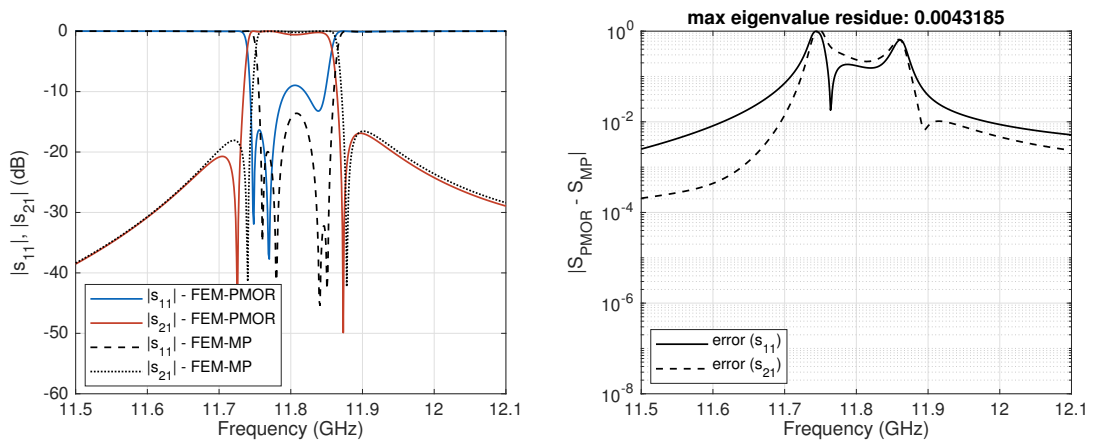


Figure 2: Results of the analysis with the **initial ROMS**.

Table 3: Values of design parameters for initial design \mathbf{p}_0 and for the analysed design \mathbf{p} .

domain	variable	\mathbf{p}_0 (mm)	\mathbf{p} (mm)
Ω_2	l_1	2.59	3.59
	l_2	2.31	3.31
Ω_3	l_x	14.30	15.30
	l_y	18.50	19.50
Ω_4	l_3	2.59	3.59
	l_4	2.31	3.31

Adding accurate eigenvectors to the projection basis

First scheme of improving the quality of ROM is to add to the projection space vectors representing eigenresonances of the macromodels. The most intuitive way is to add the eigenvectors that hit the frequency band of interest. Eigenfrequencies of all local ROMs in the frequency band 0 to 16 GHz are shown in Fig. 3. They were computed as eigenvalues of the matrix pencil $(\mathbf{\Gamma}_{\Omega_i}, \mathbf{C}_{\Omega_i})$. It can be seen that there is no eigenresonances in the frequency band of interest.

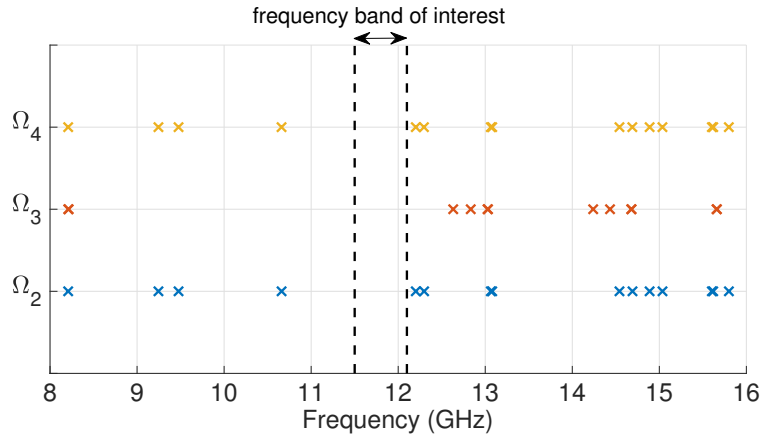


Figure 3: Spectrum of the macromodels.

We can assume that poles that are in the neighbourhood of the band of analysis are crucial in terms of accuracy of the results. Fig. 4 shows the results of the analysis when all eigenvectors up to 20 GHz were added to the basis. The scattering parameters are much more correlated with reference parameters, but the computation effort made to compute such a large number of eigenvectors is unacceptable.

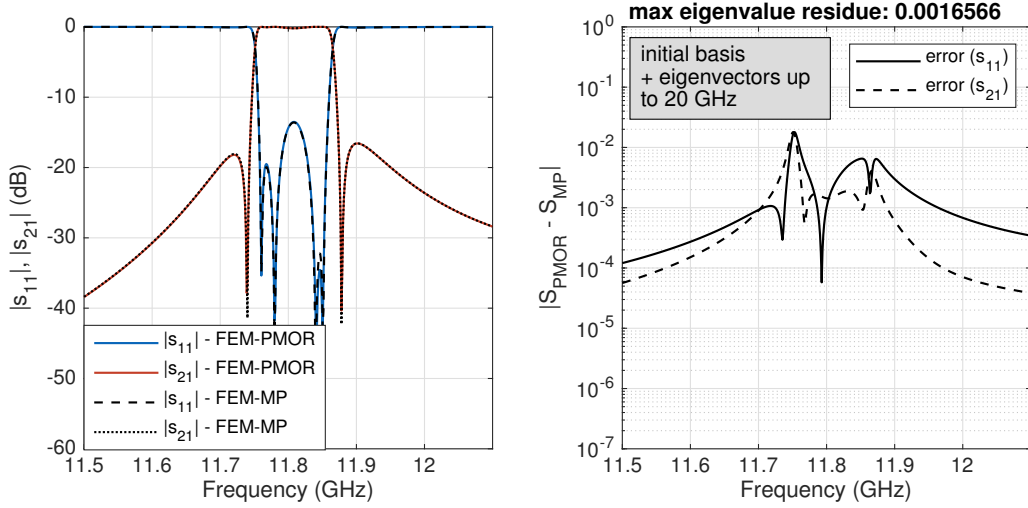


Figure 4: Scattering parameters computed with the projection basis enriched with the **eigenvectors** up to 20 GHz.

Adding snapshots to the basis

Second scheme is to improve the quality of the ROM by adding snapshots – that is vectors of the electromagnetic field in selected subdomain at the specified frequency. For this purpose, we need to define the following system of equations, based on equation 1 in which vectors of amplitudes of FE an TM modes defined at the boundaries $\mathbf{E}_{\delta\Omega_i}$ are replaced with the identity matrix \mathbf{I} (it is equivalent to the assumption that all TE and TM modes at the boundary are equally excited):

$$(\mathbf{\Gamma}_{\Omega_i} - k^2\mathbf{C}_{\Omega_i}) \cdot \bar{\mathbf{E}}_{\Omega_i} = -(\mathbf{G}_{\delta\Omega_i} - k^2\mathbf{T}_{\delta\Omega_i}) \cdot \mathbf{I} \quad (7)$$

Note that right-hand side matrix of the above equation contains multiple eigenvectors. According to Table 2, there are 82 right-hand side vectors in the system describing macromodel 2. Consequently, there are 81 and 82 right-hand side vectors in macromodel 3 and 4. Fig. 5 shows the results of uplifting all local bases with one full solution of the local systems of equation computed at the center frequency. The result is very good - the level of the actual error is approximately $1e-4$. However, the computational effort made in this step was very high due to the large number of right-hand side vectors of the local system of equations.

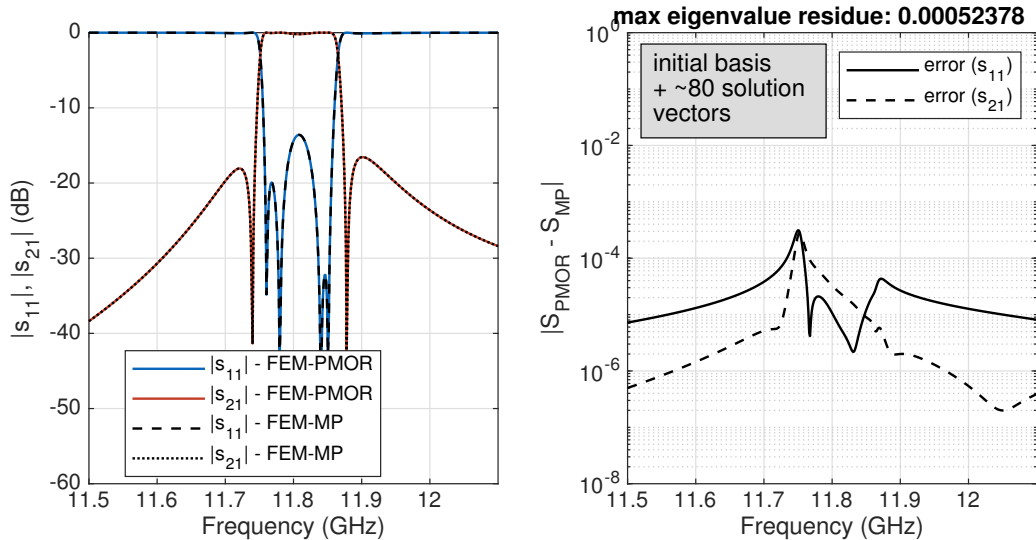


Figure 5: Scattering parameters computed with the projection basis enriched with solution vectors of for **all right-hand side vectors**.

In order to limit the computational effort, the solution of (7) can be computed only for the selected number of right-hand sides. Surely, the solution for the fundamental modes should be computed as those modes transmit the most of the energy. The measure based on the estimated error can be also used to decide if more vectors should be computed. For this purpose, the criterion based on the local error estimator may be used.

Error estimator

Local error estimator is defined in this section.

Based on the local system of equation defined in (7), equivalent reduced-order model takes the following form:

$$(\tilde{\mathbf{\Gamma}}_{\Omega_i} - k^2 \tilde{\mathbf{C}}_{\Omega_i}) \cdot \tilde{\mathbf{E}}_{\Omega_i} = -(\tilde{\mathbf{G}}_{\delta\Omega_i} - k^2 \tilde{\mathbf{T}}_{\delta\Omega_i}) \cdot \mathbf{I} \quad (8)$$

The reduced-order model is represented by the small and dense matrices $\tilde{\mathbf{\Gamma}}_{\Omega_i}, \tilde{\mathbf{C}}_{\Omega_i} \in \mathcal{R}^{r \times r}$, $\tilde{\mathbf{G}}_{\delta\Omega_i}, \tilde{\mathbf{T}}_{\delta\Omega_i} \in \mathcal{R}^{r \times m}$, where m is the number of vectors used for modal projection on the artificial boundary (number of right-hand side vectors) and r is the dimension of the reduced space.

The *a posteriori* error introduced by the MOR is based in the residual error matrix defined as:

$$\mathbf{R}(k) = (\mathbf{\Gamma}_{\Omega_i} - k^2 \mathbf{C}_{\Omega_i}) \mathbf{Q}_i \tilde{\mathbf{E}}_{\Omega_i} + (\mathbf{G}_{\delta\Omega_i} - k^2 \mathbf{T}_{\delta\Omega_i}) \mathbf{I} \quad (9)$$

where $\tilde{\mathbf{E}}_{\Omega_i}$ is a solution matrix of the local system of equations in which $\mathbf{E}_{\delta\Omega_i}$ was replaced with identity matrix \mathbf{I} . The matrix $\mathbf{R}(k) \in \mathcal{R}^{N \times m}$ contains m residual vectors, each of them corresponds to one of TE or TM modes defined at the macromodel boundary.

The estimated error is then defined as:

$$\zeta_S(k) = \mathbf{B}^T \mathbf{R}, \quad (10)$$

where \mathbf{B} is the right hand side matrix:

$$\mathbf{B}(k) = -(\mathbf{G}_{\delta\Omega_i} - k^2 \mathbf{T}_{\delta\Omega_i}) \cdot \mathbf{I} \quad (11)$$

In order to analyse the estimated error for all right-hand side vectors separately, we define the independent error estimators for all residual vectors $\mathbf{R}_i(k)$, $i = 1, \dots, m$:

$$\zeta_S^i(k) = |\mathbf{B}^T \mathbf{R}_i|_2. \quad (12)$$

Now, the values of $\zeta_S^i(k)$ can serve as a criterion to choose the residual vectors that contribute to the overall error the most. Fig. 6 shows this metric for all three macromodels.

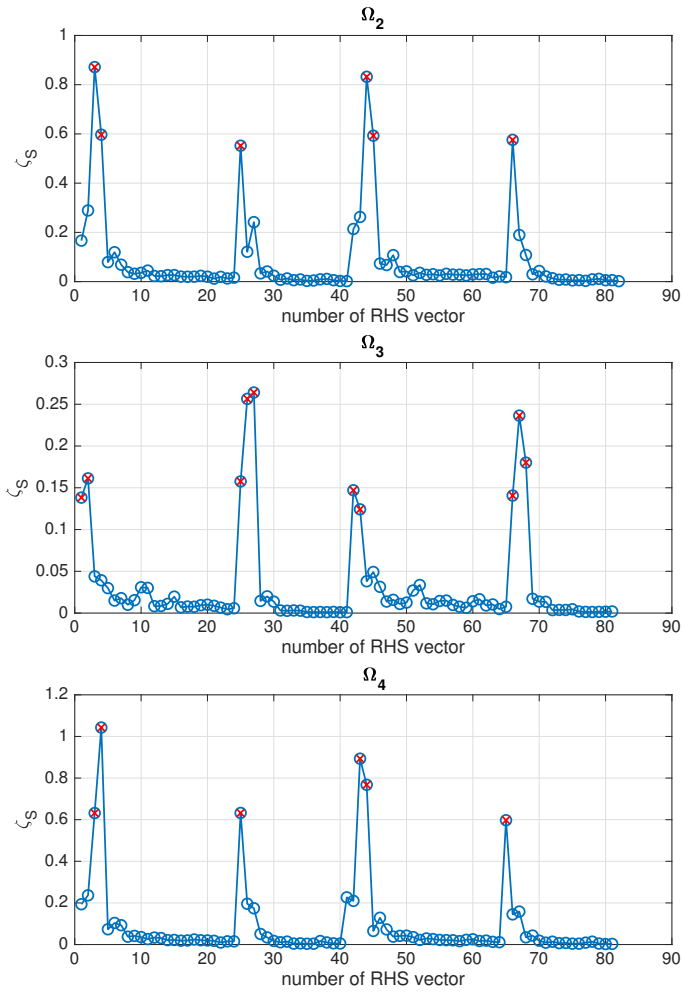


Figure 6: Estimated error computed for all the residual vectors in three macromodels. Red points - vectors with the highest value of the estimated error.

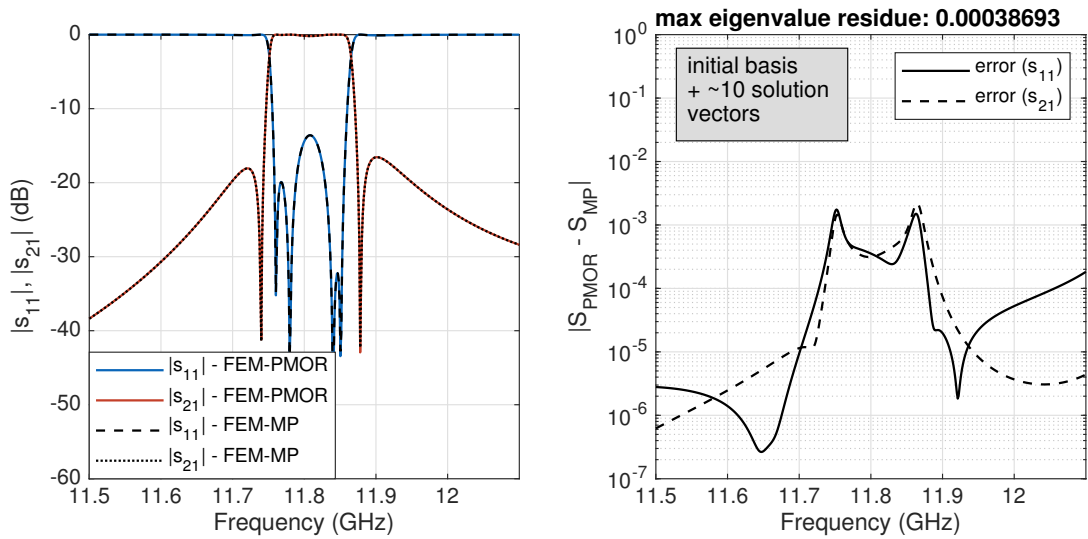


Figure 7: Scattering parameters computed with the projection basis enriched with the **limited number of solution vectors**.

Computational time

Time of generating new projection basis in all macromodels is given in Table 4. Generating new basis includes single LU factorization (using UMFPACK package) and multiple 'solve' operations for computing several block moments.

Figures 8,9,10 shows the comparison of convergence of three methods for solving linear systems of equations – preconditioned conjugate gradient (PCG), deflated preconditioned conjugate gradient (deflated PCG) and generalized minimal residual method (GMRES).

	Ω_1	Ω_2	Ω_3	Ω_4	Ω_5
time of computing new local basis (s)	11.2	28.6	22.7	27.6	9.8
number of snapshots to compute	-	10	10	10	-
number of iterations	-	28	23	22	-
time of iterative solution - def. PCG (s)	-	11.3	9.8	9.6	-

Table 4: Comparison of the execution time of the new basis generation and modification of the existing one.

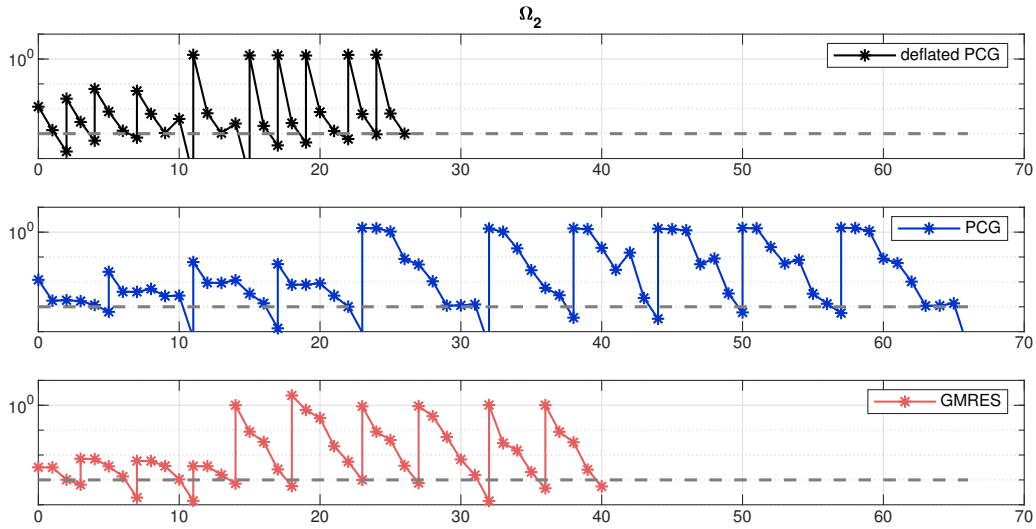


Figure 8: Convergence of PCG, deflated PCG and GMRES for solving in macromodel 2.

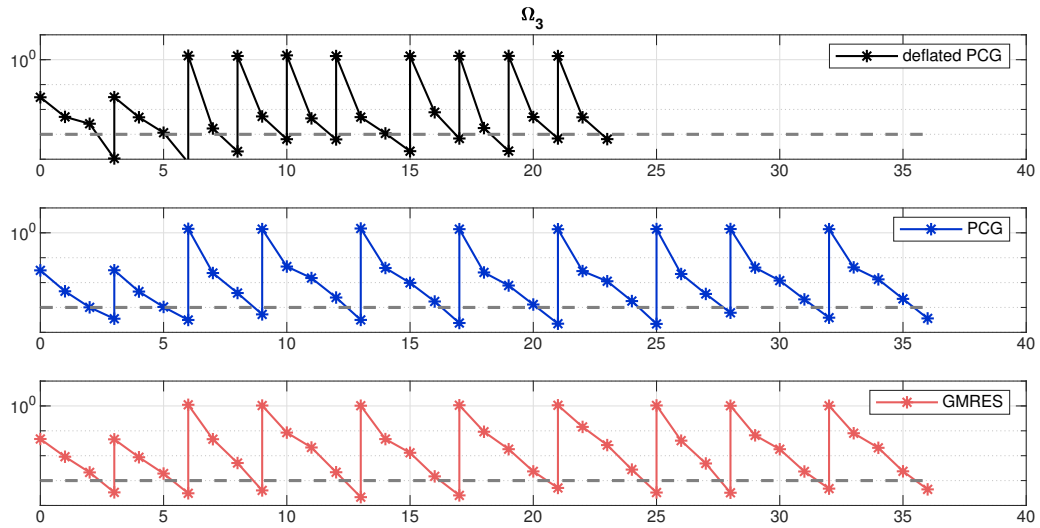


Figure 9: Convergence of PCG, deflated PCG and GMRES for solving in macromodel 3.

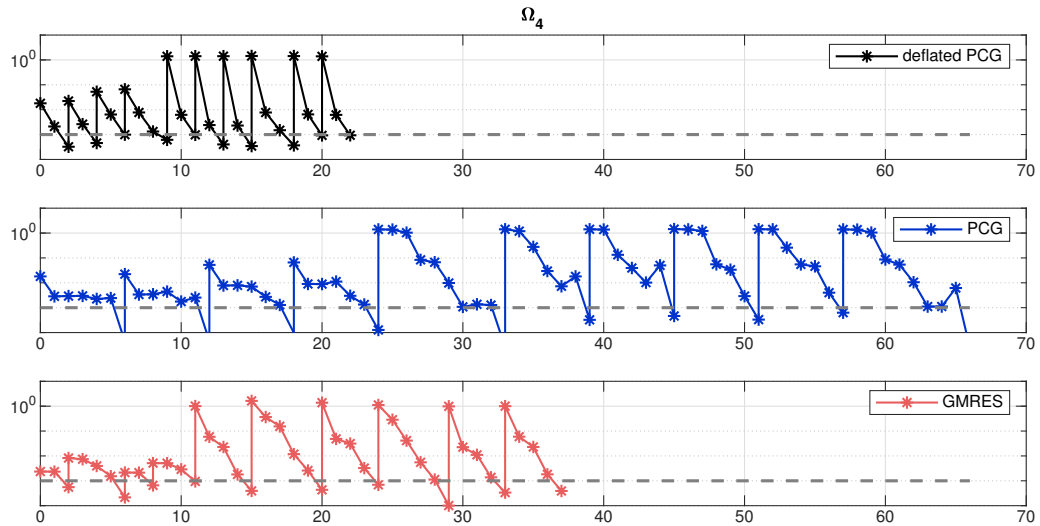


Figure 10: Convergence of PCG, deflated PCG and GMRES for solving in macromodel 4.

Summary

- The initial basis was rather poor - the change in geometry parameters (the analysed design and the 'initial' one) was quite significant, especially that the filter is very sensitive to changes in the tuning screw lengths.
- Deflated PCG converged much faster than PCG and GMRES - in all considered cases, the number of iterations was the lowest.

2.1.1 Dual mode circular waveguide filter - wideband analysis

The same filter was analysed in the wide frequency band: 11.4 - 13.4 GHz. The initial set of design parameters \mathbf{p}_0 was the same as in the narrowband analysis. However, in order to obtain desired accuracy of ROMs, the order of the ROM was higher than in the previous example. Also, the expansion frequency was different due to the different frequency band of interest.

Initial results with PMOR

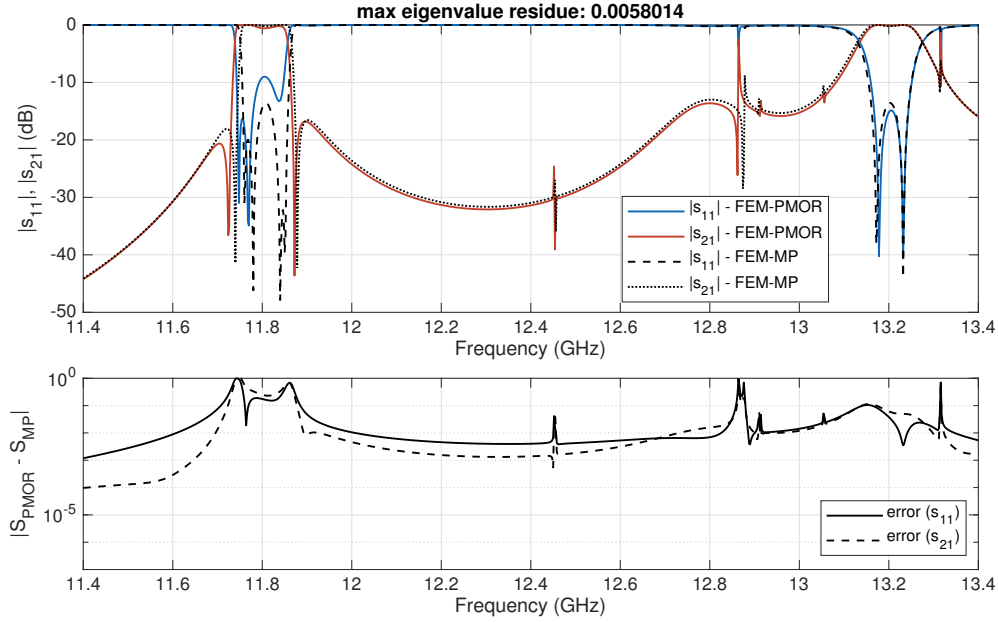


Figure 11: Scattering parameters computed with the initial PROM.

Results with uplifted PROMs

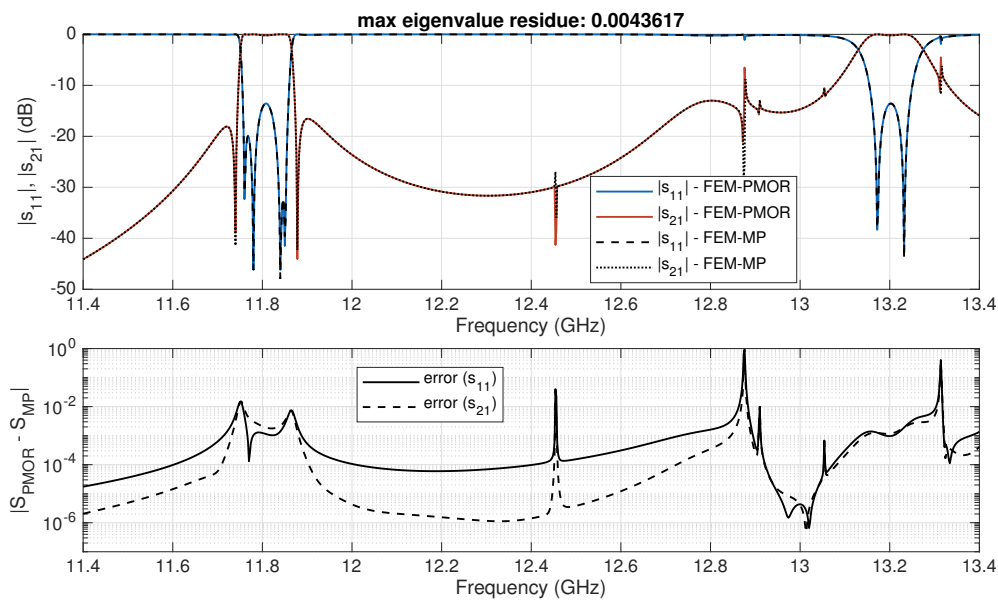


Figure 12: Scattering parameters computed with the uplifted PROM.

In this case, each of three local modes included four poles in the frequency band of interest. In total, 12 eigenvectors were computed and 23 solutions vectors of the local linear system of equation. Details on the number of vectors added to the solution space and the convergence of iterative methods is given below.

Convergence of iterative methods and computational time

	Ω_1	Ω_2	Ω_3	Ω_4	Ω_5
time of computing new local basis (s)	14.3	37.7	30.6	35.9	12.5
number of eigenvectors to compute	-	4	4	4	-
number of iterations	-	17	20	16	-
time of iterative solution - Davidson (s)	-	2.7	2.1	1.8	-
number of snapshots to compute	-	-	-	-	-
number of iterations	-	6	7	10	-
time of iterative solution - def. PCG (s)	-	6.6	7.2	10.1	-

Table 5: Comparison of the execution time of the new basis generation and modification of the existing one (wideband analysis).

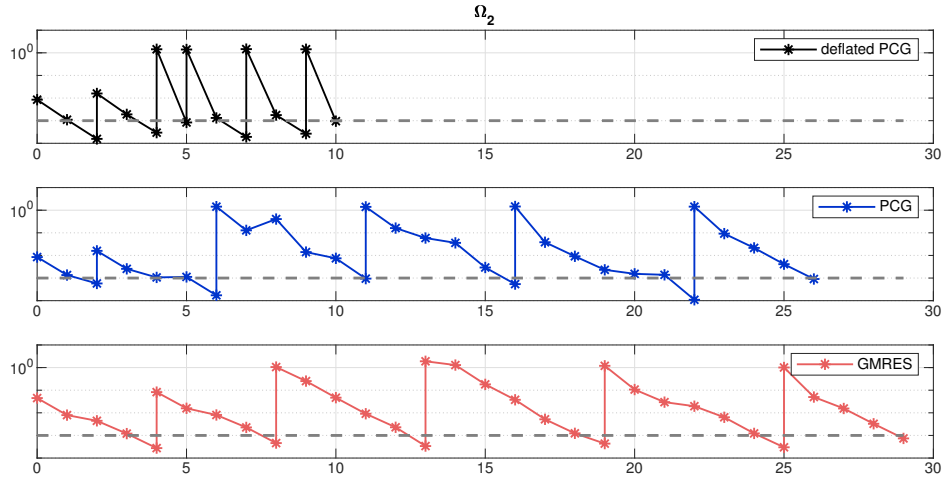


Figure 13: Convergence of PCG, deflated PCG and GMRES for solving in macromodel 2 (wideband analysis).

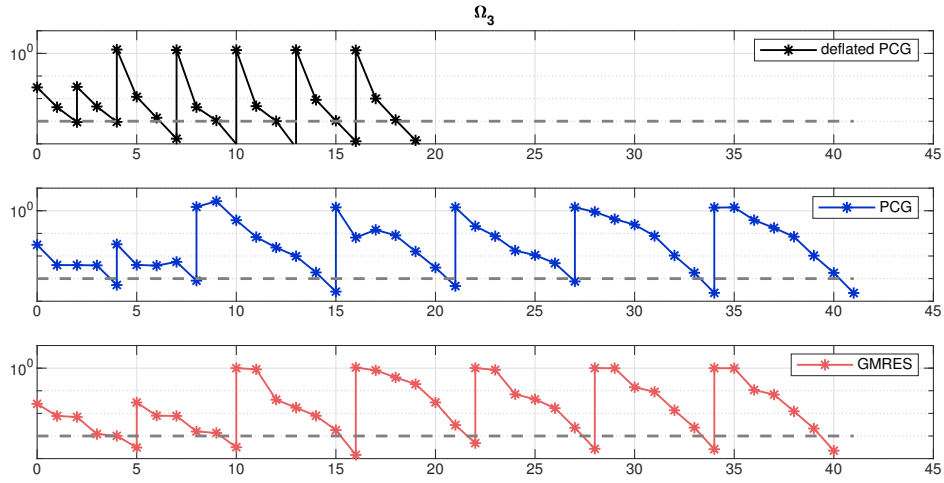


Figure 14: Convergence of PCG, deflated PCG and GMRES for solving in macromodel 3 (wideband analysis).

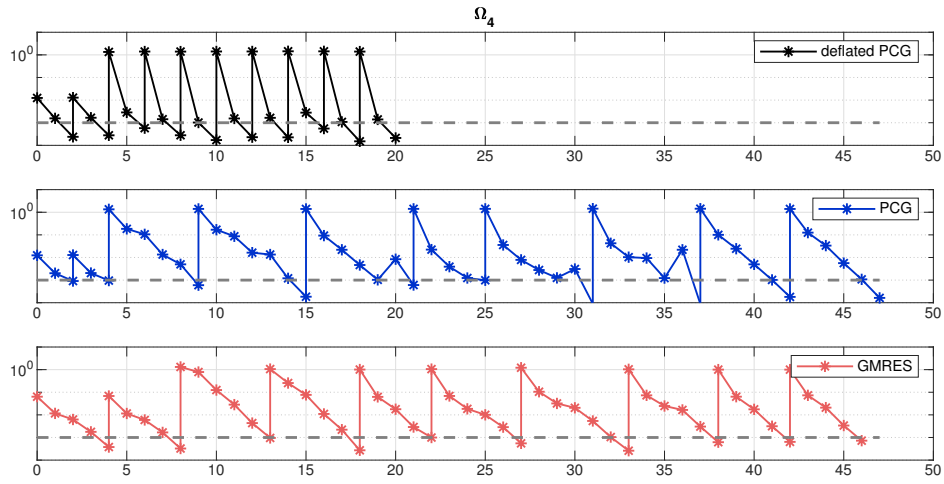


Figure 15: Convergence of PCG, deflated PCG and GMRES for solving in macromodel 4 (wideband analysis).

2.2 5th order waveguide filter

The second example is the 5th order waveguide filter. The structure was partitioned into seven subdomains $\Omega_{1,\dots,7}$ by means of six artificial boundaries $S_{1,\dots,6}$ (as shown in Fig. 16). Five subdomains were subject to the PMOR – $\Omega_{2,\dots,6}$.

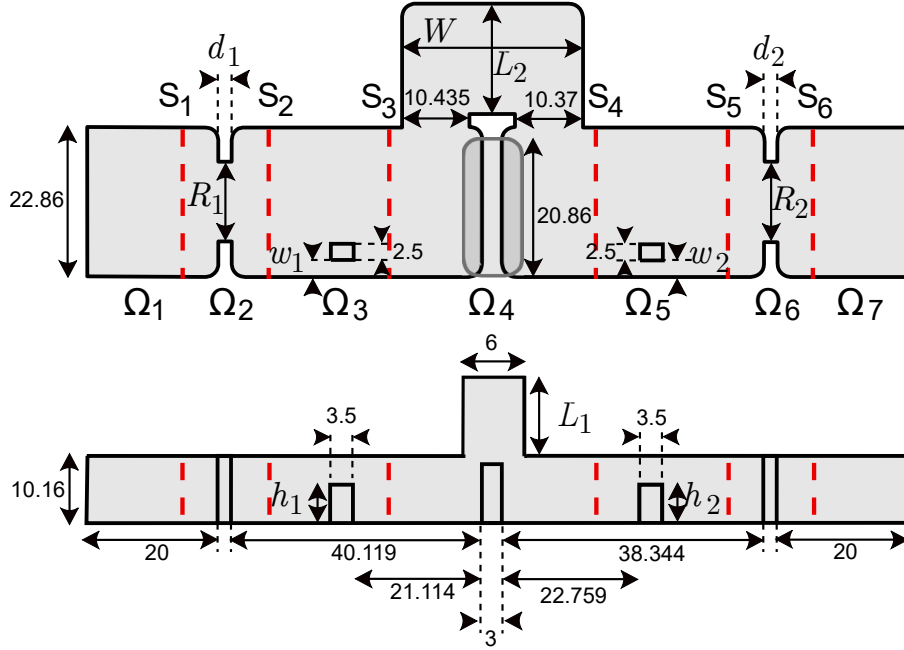


Figure 16: The structure of the filter and the segmentation scheme.

Table 6: Values of design parameters for initial design \mathbf{p}_0 and for the analysed design \mathbf{p} .

domain	variable	\mathbf{p}_0	\mathbf{p}
Ω_2	d_1	1.410	2.000
	R_1	13.624	12.188
Ω_3	h_1		5.456
	w_1		2.430
Ω_4	W	27.685	27.805
	L_1	13.444	12.194
	L_2	15.093	16.743
Ω_5	h_2		5.949
	w_2		2.430
Ω_6	d_2	0.650	2.000
	R_2	10.488	12.264

Results of the analysis with the initial PROM

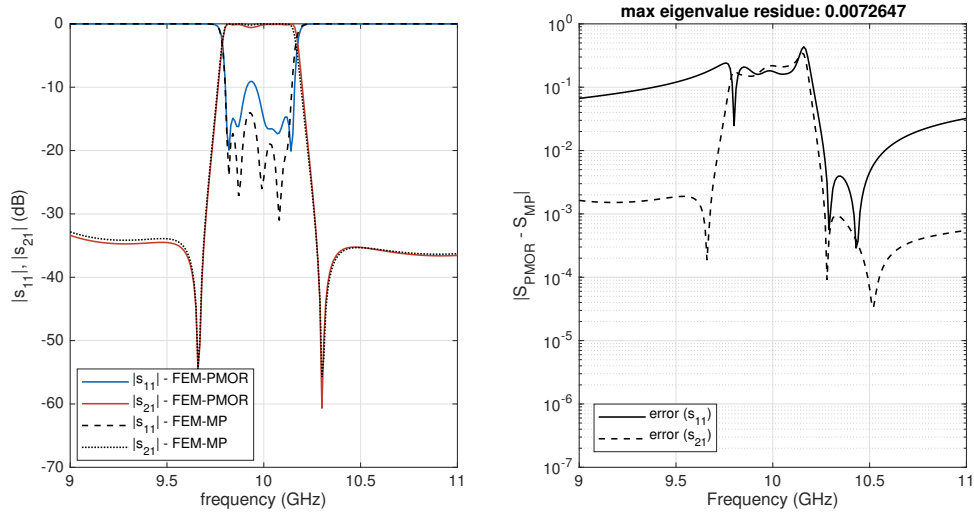


Figure 17: Scattering parameters for the initial ROM

Results of the analysis with the uplifted PROM

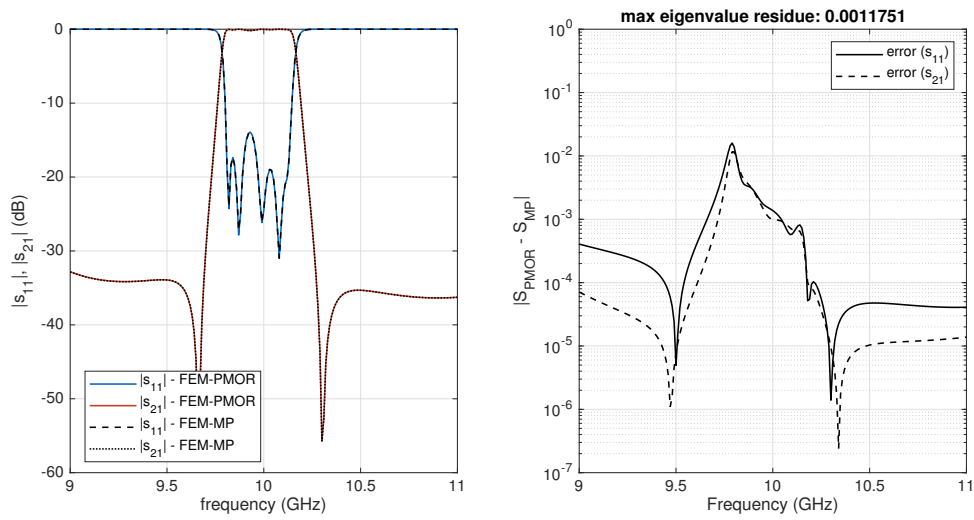


Figure 18: Scattering parameters for the uplifted ROM.

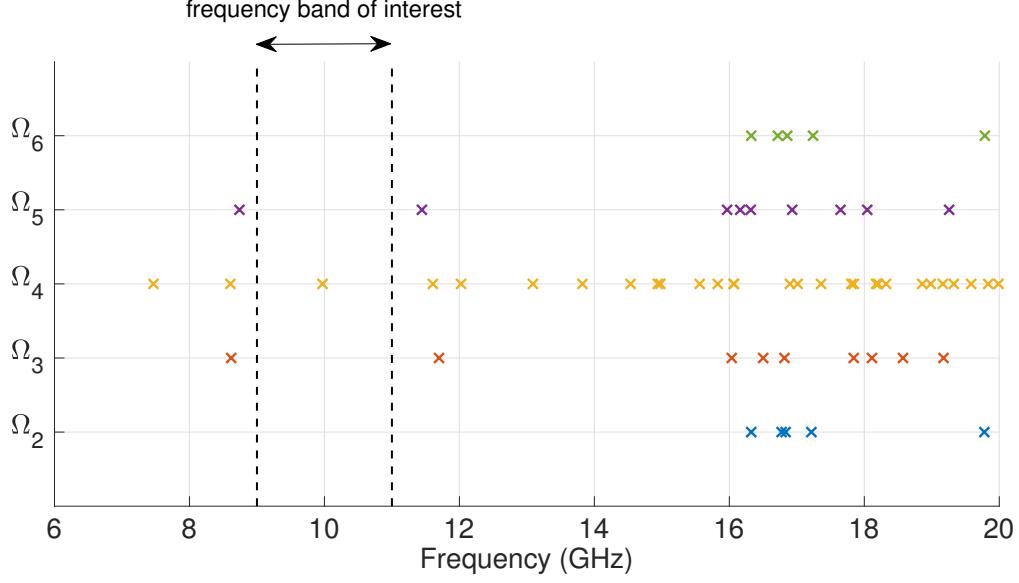


Figure 19: Eigenfrequencies of the local models.

In total, one eigenvector was computed (the pole of the macromodel 4) and 21 solution vectors of the linear system of equation. Table 7 contains time of computations: new projection basis and computing the additional vectors by means of Davidson method (for eigenproblem) and deflated PCG method (for the linear system).

	Ω_1	Ω_2	Ω_3	Ω_4	Ω_5	Ω_6	Ω_7
time of computing new local basis (s)	7.6	20.3	60.9	136.1	68.7	21.1	6.4
number of eigenvectors to compute	-	-	-	1	-	-	-
number of iterations	-	-	-	3	-	-	-
time of iterative solution - Davidson (s)	-	-	-	2.3	-	-	-
number of snapshots to compute	-	6	6	2	2	5	-
number of iterations	-	39	15	2	4	10	-
time of iterative solution - def. PCG (s)	-	7.0	12.9	9.4	4.0	4.2	-

Table 7: Comparison of the execution time of the new basis generation and modification of the existing one.

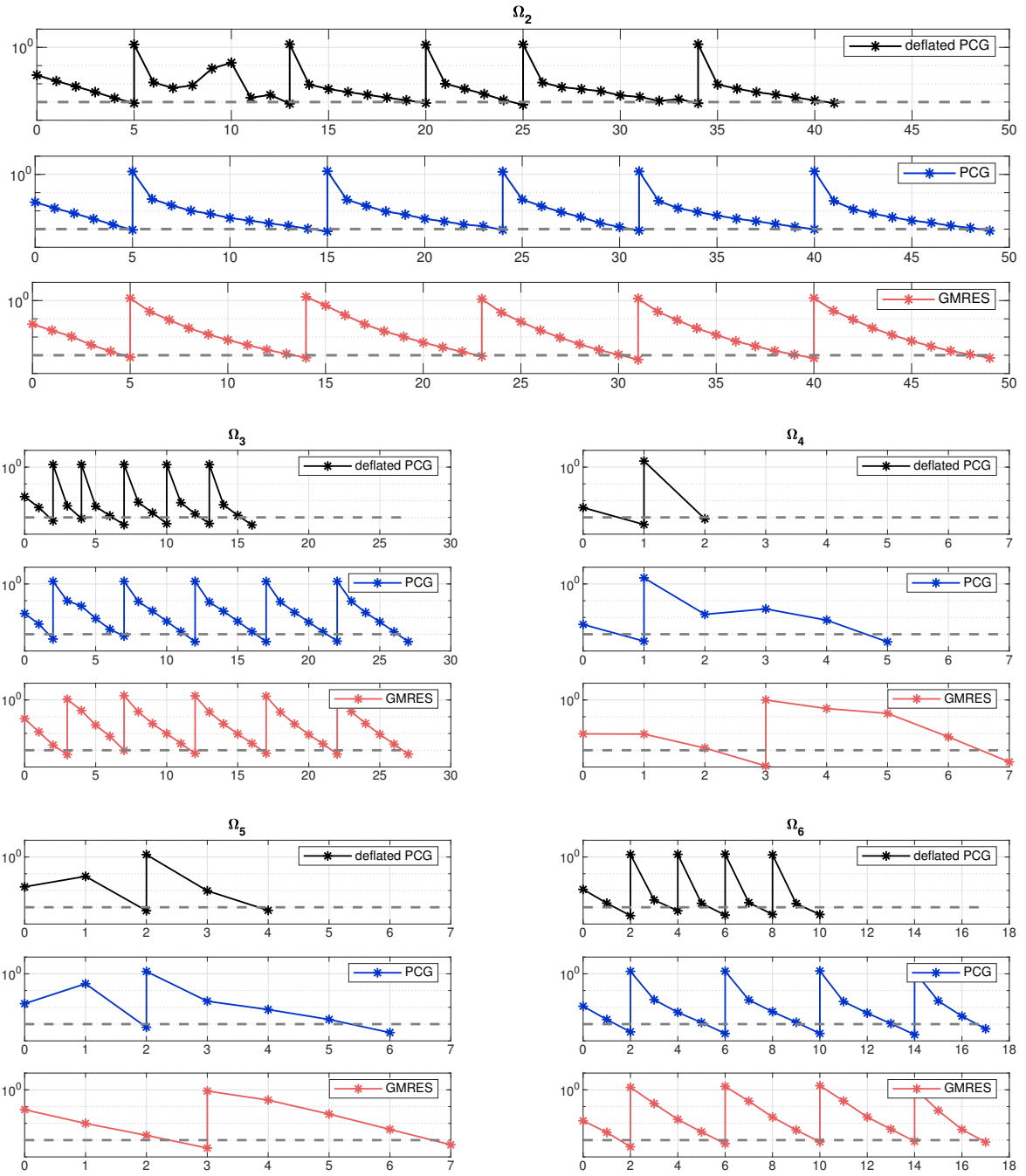


Figure 20: Convergence of iterative solvers: PCG, GMRES, deflated PCG.

References

- [1] G. Fotyga, M. Rewienski, and M. Mrozowski, "Wideband macromodels in finite element method," *IEEE Microw. Compon. Lett.*, vol. 25, no. 12, pp. 766–768, Dec. 2015.